論文 / 著書情報
Article / Book Information

題目(和文)	
Title(English)	Comparative study of renal and intestinal NaCl transporters involved in water and electrolyte homeostasis
著者(和文)	ﾘｻﾝｻﾝ
Author(English)	Shanshan Li
出典(和文)	学位:博士(理学), 学位授与機関:東京工業大学, 報告番号:甲第9238号, 授与年月日:2013年6月30日, 学位の種別:課程博士, 審査員:中村　信大,岩﨑　博史,駒田　雅之,田中　幹子,梶川　正樹,広瀬　茂久
Citation(English)	Degree:Doctor (Science), Conferring organization: Tokyo Institute of Technology, Report number:甲第9238号, Conferred date:2013/6/30, Degree Type:Course doctor, Examiner:,,,,,
学位種別(和文)	博士論文
Category(English)	Doctoral Thesis
種別(和文)	要約
Type(English)	Outline

Expression of a novel isoform of Na^+/H^+ exchanger 3 (NHE3) in the kidney and intestine of banded houndshark *Triakis scyllium*

Advisor: Professor Shigehisa Hirose

Department of Biological Sciences

Tokyo Institute of Technology

Li Shanshan

2013

CONTENTS

ABBREVIATION

NHE3	**Na^+/H^+ exchanger 3**
EnaC	epithelial sodium channel
NKCC2	Na^+-K^+-$2Cl^-$ cotransporter 2
NCC	Na^+-Cl^- cotransporter
TAL	renal thick ascending limb
DCT	distal convoluted tubule
TMAO	trimethylamine oxide
DMEM	Dulbecco's modified Eagle’s medium
FBS	fetal bovine serum
PBS	phosphate buffered saline
PCR	polymerase chain reaction

SUMMARY

NHE3 provides one of the major Na^+ absorptive pathways of the intestine and kidney in mammals, and recent studies of aquatic vertebrates (teleosts and elasmobranchs) have demonstrated that NHE3 is expressed in the gill and plays important roles in ion and acid-base regulation. To understand the role of NHE3 in elasmobranch osmoregulatory organs, I analyzed renal and intestinal expressions and localizations of NHE3 in a marine elasmobranch, Japanese banded houndshark (*Triakis scyllium*). mRNA for *Triakis* NHE3 was most highly expressed in the gill, kidney, spiral intestine, and rectum. The kidney and intestine expressed a transcriptional isoform of NHE3 (NHE3k/i), which has a different amino terminus compared to that of NHE3 isolated from the gill (NHE3g), suggesting that NHE3k/i and NHE3g arise from a single gene by alternative promoter usage. Immunohistochemical analyses of the *Triakis* kidney demonstrated that NHE3k/i is expressed in the apical membrane of a part of the proximal and late distal tubules in the sinus zone. In the bundle zone of the kidney, NHE3k/i was expressed in the apical membrane of the early distal tubules known as the diluting segment. In the spiral intestine and rectum, NHE3k/i was localized towards the apical membrane of the epithelial cells. The transcriptional levels of NHE3k/i were increased in the kidney when *Triakis* was acclimated in 130% seawater, whereas those in the spiral intestine were increased in fish acclimated in diluted seawater. These results suggest that NHE3 is involved in renal Na^+ reabsorption, urine acidification, and intestinal Na^+ absorption in elasmobranchs.

MATERIALS AND METHODS

Antibodies. Rat polyclonal antisera against 212 amino acids of the carboxyl tail of Atlantic stingray NHE3 that was developed by Choe *et al.* (12) and a serum R1B2, that yields the highest signal-to-background ratios, were used in the present analysis. Rabbit polyclonal antiserum against eel Na^+-K^+-ATPase α-subunit (amino acid residues 469–773) was prepared by Mistery *et al*. (35).

Experimental animals. The animal protocols and procedures were approved by the Institutional Animal Care and Use Committees of Tokyo Institute of Technology and the University of Tokyo and conform to the American Physiological Society's “Guiding Principles in the Care and Use of Laboratory Animals” (1). Japanese banded houndshark, *Triakis scyllium*, were collected in Koajiro Bay, Kanagawa, Japan. They were transported to the Atmosphere and Ocean Research Institute and kept in 2×10^3 L holding tanks (20–22°C, aerated) under a constant photoperiod (12 h:12 h, L:D). The fish were fed on squid for at least 2 weeks before experiments. To examine the effects of environmental salinity on NHE3 mRNA expression, the fish were transferred to diluted (60%) or concentrated (130%) seawater as described previously (21). For sampling, fish were anesthetized with 0.02% (w/v) 3-aminobenzoic acid ethyl ester (Sigma, St Louis, MO, USA) (46).

RNA isolation and molecular cloning. Houndsharks were anesthetized with fish-culture water containing tricaine methanesulfonate (MS-222, 200–500 mg/l)

(Nacalai Tesque, Kyoto, Japan) and the brains, gills, kidneys, spleens, livers, rectums, spiral intestine, rectal glands, skin, muscles, and blood were collected. Total RNA was isolated from the tissues using the acid guanidinium thiocyanate-phenol-chloroform extraction method with Isogen (Nippon Gene, Tokyo, Japan) (37). Concentration and quality of RNA were measured on the basis of UV absorbance at 260 nm and 280 nm and checked using denaturing agarose gel electrophoresis.

To clone partial sequences, cDNAs were synthesized using SuperScript III first-strand synthesis system (Invitrogen, Carlsbad, CA, USA). Degenerate primer pairs designed by Choe et al. (Table 1) (12) were used to amplify conserved regions of NHE. Each PCR was performed with Ex Taq HS DNA polymerase (Takara Bio). PCR products were purified by 1.2% agarose gel, ligated into a pGEM-T vector, and transformed into DH5α competent cells (Invitrogen). Plasmid DNA was then sequenced in both directions.

Full-length cDNAs for NHE3k/i (renal and intestinal isoform) and NHE3g (gill isoform) were obtained by rapid amplification of cDNA ends (RACE) using the First Choice RLM-RACE kit (Ambion, Austin, TX, USA) from the kidney and gill of *Triakis scyllium*, respectively, with the primers in Table 1. The sequences were assigned EMBL/GenBank/DDBJ accession numbers AB632345 (NHE3k/i) and AB632346 (NHE3g).

Sequence analysis of Triakis NHE3k/i and NHE3g. Sequences obtained by initial degenerate primer pairs were assembled, and the resulting contig amino acid translations were analyzed with the basic local alignment search tool

(BLAST) on the National Center for Biotechnology Information website (http://www.ncbi.nlm.nih.gov/). Full-length cDNA sequences for NHE3k/i and NHE3g were assembled with Genetyx software (Genetyx, Tokyo, Japan) and the assembled nucleotide sequence was searched for open reading frames. The predicted amino acid sequence was aligned with NHE3 sequences from *Homo sapiens* (human, accession number NM_004174), *Mus musculus* (mouse, NM_001081060), *Rattus norvegicus* (rat, NM_012654), *Dasyatis sabina* (Atlantic stingray, AY626250), *Danio rerio* (zebrafish, NM_001113473 and NM_001113479), and *Tribolodon hakonensis* (Japanese dace, AB055466) using Clustal W software. MEGA software (47) was used to make a phylogenetic tree by the neighbor-joining method (43) and Poisson-corrected evolutionary distances. Branches were then tested for statistical significance by bootstrapping with 2,000 replicates. The expected locations of membrane-spanning regions and regions important for regulation of the transporter were taken from previously published reports or predicted using Genetyx software and ExPASy tools (http://www.expasy.org/tools/).

Semi-quantitative reverse transcription (RT)-PCR. Semi-quantitative RT-PCR was performed as described previously (49). Five micrograms of total RNAs prepared from houndshark tissues were reverse-transcribed using the SuperScript III first-strand synthesis system. cDNA (125 nl of the SuperScript III reaction) was used as the template for PCRs with specific primers in Table 1. Each reaction consisted of 200 ng of cDNA, 0.2 μM each primer, 12.5 μl of 2 × GoTaq Green master mix (Promega), and nuclease-free water in a final volume

of 25 μl. The PCR conditions were as follows: 29 or 32 cycles of denaturation (94°C, 15 s), annealing (55°C, 30 s), and extension (72°C, 1 min). After PCR amplification, 10 μl of each reaction mixture was run on a 1.2% agarose gel. The gel was stained with 0.5 μg/ml ethidium bromide, and the fluorescence image analyzed with a Kodak Image Station 2000R system (Eastman Kodak, Rochester, NY, USA).

Quantitative real-time RT-PCR. Quantification of mRNA levels by real-time PCR was described in detail previously (56). To compare expression levels of NHE3k/i and NHE3g in the gill, kidney, spiral intestine, and rectum, partial cDNA fragments of NHE3k/i, NHE3g, GAPDH, and β-actin were amplified by PCR from plasmids containing full-length cDNA. Total RNA was extracted from the gill, kidney, spiral intestine, and rectum using Isogen (Nippon Gene), and 5 μg of RNA was used as a template for the reverse transcription using the SuperScript III first-strand synthesis system. Real-time PCR was performed with a Thermal Cycler Dice Real-Time System (Takara Bio). The PCR mixture (25 μl) contained SYBR Premix Ex Taq II Kit (Takara Bio), 400 nM forward and reverse primers (Table 1), and standard cDNA (10^{-4}–10^{-11} ng/reaction) or 125 nl of reverse-transcribed cDNA samples. The specificity of the method was confirmed by a dissociation analysis. To examine the effects of environmental salinity on NHE3 mRNA expression, the reverse-transcribed cDNA samples of the kidney or spiral intestine of the control fish were pooled and used as standards. The PCR mixture (25 μl) contained SYBR Premix Ex Taq II Kit, 400 nM forward and reverse primers (Table 1), and standard cDNA (125–1 nl/reaction) or 125 nl of

reverse-transcribed cDNA samples from fish transferred to diluted (60%), concentrated (130%), or control (100%) seawater. Data were expressed as means ± SE, and statistically analyzed by ANOVA followed by the Tukey-Kramer test using the GraphPad Prism software (GraphPad, San Diego, CA).

Cell culture, transfection and immunocytochemistry. Antibody specificity was established by staining COS7 (SV40-transformed African green monkey kidney fibroblast cell line) cells exogenously expressing *Triakis* NHE3k/i and NHE3g proteins. Full-length cDNA for NHE3k/i or NHE3g was subcloned into the p3×FLAG-CMV10 vector (Sigma-Aldrich). COS7 cells were cultured in DMEM (Sigma-Aldrich) containing 10% FBS, 100 U/ml penicillin, and 100 μg/ml streptomycin. The cells were transfected with plasmids encoding FLAG-NHE3k/i or an empty vector (mock transfection) using Lipofectamine LTX (Invitrogen), according to the manufacturer's instructions.

For immunofluorescence experiments, the cells were fixed with 2% paraformaldehyde (PFA) in 0.1 M phosphate buffer (pH 7.4) at 4°C for 10 min, permeabilized with 0.1% Triton X-100 in PBS at 4°C for 10 min, and blocked with 5% FBS in PBS for 1 h at room temperature. After blocking, the cells were stained by anti-NHE3 antiserum (1:1,000 dilution), with or without mouse M2 anti-FLAG monoclonal antibodies (2 μg/ml, Sigma-Aldrich), for 1.5 h at room temperature followed by Alexa Fluor 488- and 546-labeled secondary antibodies (1:2,000 dilution; Invitrogen) for 1 h at room temperature. Nuclei were stained with Hoechst 33342 (100 ng/ml; Invitrogen). Fluorescence images were

obtained with a laser confocal microscope (TCS-SPE; Leica, Wetzlar, Germany) using a fixed setting and processed with LAS AF software (Leica).

Expression and immunohistochemistry of NHE3k/i and NHE3g in Xenopus *oocytes.* The entire coding regions of *Triakis* NHE3k/i and NHE3g cDNAs were inserted into the pGEMHE *Xenopus laevis* expression vector (28, 55). The plasmids were linearized with *Not* I, and cRNAs transcribed in vitro using the T7 mMessage mMachine kit (Ambion). *X. laevis* oocytes were dissociated with collagenase as previously described (42) and injected with 50 nl of water or a solution containing cRNA at 0.5 g/L (25 ng/oocyte). Oocytes were incubated at 16°C in OR3 medium, and studied 3–4 days after injection. The oocytes were washed in ND96 medium, fixed in 2% PFA in 100 mM phosphate buffer (pH 7.4) at 4°C for 1 h, and washed in ND96. The ND96 medium contained 96 mM NaCl, 2 mM KCl, 1 mM $MgCl_2$, 1.8 mM $CaCl_2$, and 5 mM HEPES (pH 7.5). The oocytes were then quickly frozen in an optimum cutting temperature compound (Sakura Finetek, Tokyo, Japan). Frozen sections (6 μm) were prepared, permeabilized with 0.1% Triton X-100 in PBS at 20°C for 10 min, incubated with 5% FBS (Invitrogen) in PBS at 20°C for 1 h, and incubated with rat anti-NHE3 antiserum (1:1,000) (12) in PBS containing 5% FBS at 20°C for 16 h. After washing with PBS, the sections were incubated with Alexa Fluor 488-labeled secondary antibody (1:2,000 dilution) in PBS containing 5% FBS at 20°C for 1 h. The sections were mounted on antifade glycerol (90% glycerol, 10% 10× PBS, and 0.1% 1,4-phenylenediamine at pH 7.4). Fluorescence images were obtained with a laser confocal microscope as described above.

Immunohistochemistry of shark tissues. Kidney, spiral intestine, and rectum from *Triakis scyllium* were fixed in 4% PFA in 100 mM phosphate buffer (pH 7.4) at 4°C for 2 h, and rinsed in PBS containing 7% sucrose. The tissues were cryoprotected through a series of increasing sucrose concentrations up to 20% and quickly frozen in an optimum cutting temperature compound. Frozen sections (6 μm) were prepared, permeabilized with 0.1% Triton X-100 in PBS at 20°C for 10 min, incubated in PBS containing 5% FBS (Invitrogen) at 20°C for 1 h. They were then incubated with rat anti-NHE3 antiserum (1:1,000) (12) and rabbit anti-NaK-ATPase antiserum (1:1000) (35) in PBS containing 5% FBS at 20°C for 16 h. After washing with PBS, the sections were incubated with Alexa Fluor 488- and 594-labeled secondary antibodies (1:2,000 dilution), tetramethylrhodamine isothiocyanate (TRITC)-labeled phalloidin (0.15 μM; Sigma-Aldrich), and Hoechst 33342 (100 ng/ml) in PBS containing 5% FBS at 20°C for 1 h. The sections were mounted on antifade glycerol, and fluorescence images were obtained with a laser confocal microscope as described above.

RESULTS

Molecular cloning and tissue distribution of NHE3k/i and NHE3g in banded houndshark. Degenerate primers designed by Choe et al. (12) to anneal conserved region of the amino acid sequences of NHEs in various species were also used in this study to obtain a partial cDNA fragment of *Triakis* NHE3 from the kidney by RT-PCR. BLAST search and a phylogenetic analysis of the deduced amino-acid sequence of the PCR product confirmed that the PCR product was the *Triakis* ortholog of NHE3 (data not shown). In the sequence, I designed another set of primers having 100% match with *Triakis* NHE3 (F1/R1, Fig. 1A) and used them for tissue distribution analysis by semi-quantitative RT-PCR. Within 11 tissues tested, a relatively high-level expression was observed in the gill, kidney, and intestines (spiral intestine and rectum) with intermediate or low-level of expression in various other tissues (Fig. 1B, upper panel for F1/R1 primers). This pattern of expression is similar to that of NHE3 in Atlantic stingray (12).

Full-length cDNA for *Triakis* NHE3 was isolated initially from the kidney by 5'- and 3'-RACE. When I designed another set of primers in the 5' end (F3/R2, Fig. 1A) and repeated the tissue distribution analysis, it exhibited a strong band only in the kidney and intestines (spiral intestine and rectum) but not the gill and other tissues (Fig. 1B, the third panel for F3/R2 primers). These results indicated that (i) the isolated cDNA for NHE3 is the kidney and intestine isoform (NHE3k/i), and (ii) the gill expresses another transcriptional isoform of NHE3 (NHE3g). I

next isolated *Triakis* NHE3 from the gill by 5'- and 3'-RACE again. The sequence of the full-length cDNA for NHE3 from the gill (NHE3g) was identical with NHE3k/i except for the 5' end. I designed another set of primers in the 5' end of NHE3g (F2/R2, Fig. 1A), and repeated the tissue distribution analysis (Fig. 1B). NHE3g was expressed mainly in the gill with intermediate or low-level of expression in various other tissues (Fig. 1B, the second panel for F2/R2 primers). These results indicate that NHE3k/i and NHE3g are transcribed from a single gene by alternative promoter usage.

Dominant expressions of NHE3k/i in the kidney and intestine (spiral intestine and rectum) and NHE3g in the gill were confirmed by quantitative real-time RT-PCR (Fig. 1C). GAPDH was used as a reference gene. The kidney, spiral intestine, and rectum expressed 40–300 times more NHE3k/i than NHE3g. In the gill, the level of NHE3g expression was ~10 times higher than that of NHE3k/i.

Primary structure of NHE3k/i and NHE3g. cDNAs for NHE3k/i and NHE3g contain open reading frame codings for an 826- and 832-amino-acid polypeptide, respectively, that are identical for the most part except for the 78- or 84-amino-acid-residue in the amino termini, respectively, which share only a 37% identity (blue line in Fig. 2). Amino acid sequence of the common region (749 amino acid residues) of *Triakis* NHE3s shared 88, 73, 74, 48, 52, and 48% identities with those of Atlantic stingray NHE3 (12), human NHE3 (7), mouse NHE3 (41), Japanese dace NHE3 (19), zebrafish NHE3a (57), and zebrafish NHE3b (57), respectively. Amino terminus of *Triakis* NHE3k/i (78 amino acid

residues) was 28, 26, 27, 21, 29, and 23% identical to those of Atlantic stingray NHE3, human NHE3, mouse NHE3, Japanese dace NHE3, zebrafish NHE3a, and zebrafish NHE3b, respectively; and the amino terminus of *Triakis* NHE3g (84 amino acid residues) shared 62, 30, 27, 27, 31, and 21% identity with those of Atlantic stingray NHE3, human NHE3, mouse NHE3, Japanese dace NHE3, zebrafish NHE3a, and zebrafish NHE3b, respectively.

Multiple alignments of NHE3s of various species are shown in Fig. 2. The alternative amino termini of *Triakis* NHE3k/i and NHE3g were both homologous to the first coding exon of the NHE3 genes of other species (arrowhead in Fig. 2): human NHE3 (Ensembl gene ID: ENSG00000066230), rat (ENSRNOG00000015159 (22)), mouse NHE3 (ENSMUSG00000036123), zebrafish NHE3a (ENSDARG00000058498), and zebrafish NHE3b (ENSDARG00000036722), suggesting that the *Triakis* NHE3 gene has two exon 1s that are regulated differentially by each promoter. Hydropathy plot in combination with a signal peptide prediction tool showed that both alternative amino termini of *Triakis* NHE3s code for a putative signal peptide and a half of the first transmembrane domain. Putative 11 transmembrane domains and consensus sequences for phosphorylation are marked in Fig. 2.

Phylogenetic analysis. Amino acid sequences of the common region (749-amino-acid-residue) or alternative amino termini of *Triakis* NHE3s were aligned with those of NHE3s in various species, and a phylogenetic tree was generated by the Neighbor–Joining method (43) (Fig. 1, *D* and *E*). The phylogenetic tree generated with the common region confirmed the orthologous

relationship between *Triakis* NHE3s and the others. In the phylogenetic tree of the exon 1 coding region, *Triakis* NHE3g formed an individual branch with Atlantic stingray NHE3.

Antibody cross-reactivity. Antibody against Atlantic stingray NHE3 (RIB2) had been raised by Choe et al. (12) and successfully used for immunohistochemical studies of the gills of Atlantic stingray and other elasmobranch species, spiny dogfish shark (*Squalus acanthias*) (10) and Japanese banded houndshark (*Triakis scyllium*) (46). In the present study, 3×FLAG-tagged *Triakis* NHE3k/i and NHE3g were expressed in COS7 cells and the cross-reactivity of the antibody was examined. Expressions of the FLAG-tagged proteins were confirmed using anti-FLAG antibody. Anti-stingray NHE3 rat antiserum (RIB2) and anti-FLAG antibody stained COS7 cells expressing 3×FLAG-NHE3k/i or 3×FLAG-NHE3g but not mock-transfected cells (Fig. 3, *A*–*C*). The signal was not detected when cells were stained with normal rat serum. These results demonstrated that anti-stingray NHE3 rat antiserum RIB2 cross-reacts with *Triakis* NHE3k/i and NHE3g. The antibody also labeled *Xenopus* oocytes injected with cRNAs for *Triakis* NHE3k/i and NHE3g, but not water-injected oocytes (Fig. 3*D*). No clear difference was observed in the staining patterns between NHE3k/i and NHE3g oocytes (n = 6 for each group).

Immunohistochemical analysis of the kidney. The *Triakis* kidney consists of two zones: the bundle zone and the sinus zone (20, 29). In frozen sections of the *Triakis* kidney, NHE3 specific signals were detected in the apical membrane of

renal tubules in both the bundle and sinus zones (Fig. 4). No signal was obtained with the preimmune serum (Fig. 4, *C* and *I*).

In the bundle zone, five tubular segments are arranged to form countercurrent loops in the peritubular sheath (dotted lines in Fig. 4, *A* and *B*). Specific signals for NHE3 were detected in the apical membrane of one of the five tubules (Fig. 4, *A* and *B*). The NHE3 positive tubules in the bundle zone with relatively large diameters and consisting of relatively tall epithelial cells, showed weak luminal staining by phalloidin (i.e., no brush border) (Fig. 4, *B* and *E*), and stained strongly with anti-Na^+/K^+-ATPase (Fig. 4, *A* and *D*). These results clearly indicate that NHE3 is expressed in the early distal tubule of the ascending limb of the third loop (intermediate IV segment as designated by Lacy and Reale) (29).

The sinus zone roughly consists of the 2nd (proximal tubules and intermediate tubules) and 4th (late distal tubules) loops. The proximal tubules were identified by a large diameter, tall epithelium, the presence of a brush border, and shallow basal infolding that stained with anti-Na^+/K^+-ATPase antibody. The late distal tubules were identified by a small diameter, thin epithelium, absence of a brush border, and deep basal infolding of the basolateral membrane which that stained strongly with anti-Na^+/K^+-ATPase antibody. In the sinus zone of *Triakis* kidney, specific signals for NHE3 were detected in a part of the proximal and late distal tubules. In other words, NHE3 positive and negative segments were both observed in each tubule (Fig. 4, F–K). NHE3 negative proximal tubules were frequently seen in the sinus zone near the bundle zone (Fig. 4*F*).

Immunohistochemical analysis of the intestine. The luminal surface of the *Triakis* spiral intestine, the major part of the intestine, was covered by tall columnar epithelial cells. Immunohistochemical analysis of frozen sections for the spiral intestine showed that NHE3 is expressed in the apical membrane of absorptive epithelial cells (Fig. 5*A*). NHE3 positive signal was similarly observed in the apical membrane of rectal epithelium (Fig. 5*C*). No significant signal was obtained with the preimmune serum (Fig. 5, *B* and *D*).

Environmental salinity dependent expression of NHE3k/i. Renal and intestinal expressions of NHE3k/i were compared among sharks acclimated to 100% (control), 60% (low), or 130% (high) seawater. In the high salinity group, renal expression of NHE3k/i was significantly increased compared with the low salinity group (Fig. 6, $p < 0.05$, $n = 4–8$). In contrast, intestinal expression of NHE3k/i was significantly increased in the low salinity group compared with the high salinity group (Fig. 6, $p < 0.05$, $n = 4–8$).

FIGURES

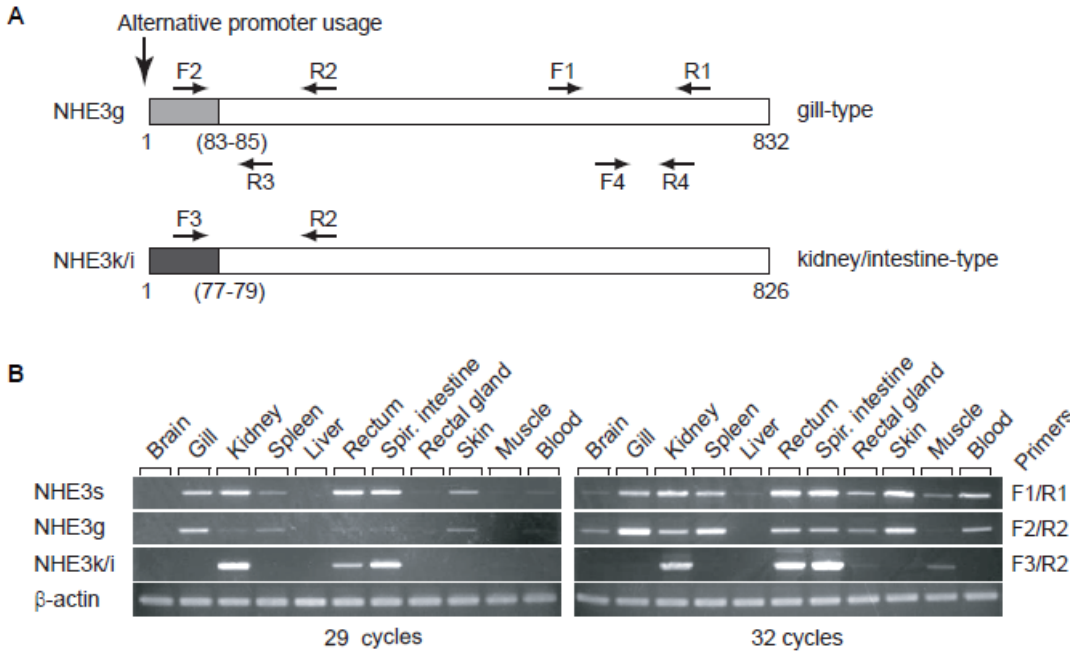
A
Alternative promoter usage
F2
R2
F1
R1
NHE3g
gill-type
1
(83-85)
832
R3
F4
R4
F3
R2
NHE3k/i
kidney/intestine-type
1
(77-79)
826
B
Brain
Gill
Kidney
Spleen
Liver
Rectum
Spir. intestine
Rectal gland
Skin
Muscle
Blood
Primers
NHE3s
NHE3g
NHE3k/i
β-actin
F1/R1
F2/R2
F3/R2
29 cycles
32 cycles

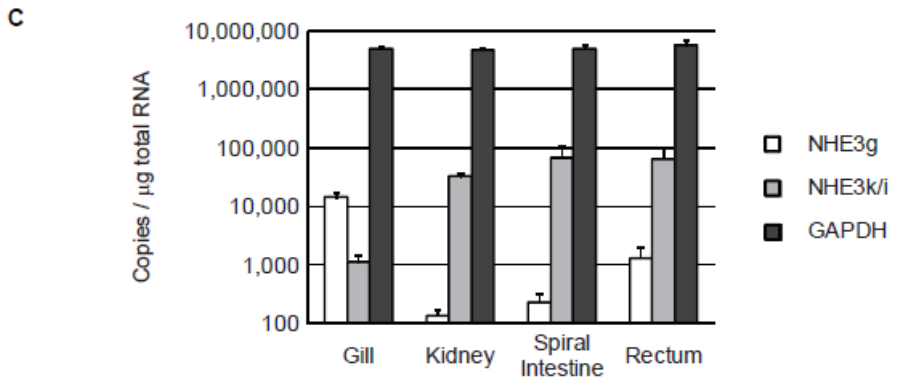
C
Copies / µg total RNA
10,000,000
1,000,000
100,000
10,000
1,000
100
Gill
Kidney
Spiral Intestine
Rectum
NHE3g
NHE3k/i
GAPDH

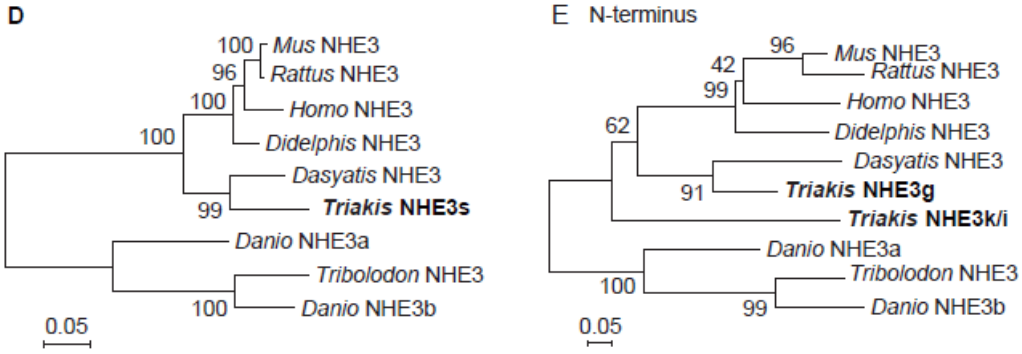
D
100
Mus NHE3
96
Rattus NHE3
100
Homo NHE3
100
Didelphis NHE3
Dasyatis NHE3
99
Triakis NHE3s
Danio NHE3a
Tribolodon NHE3
100
Danio NHE3b
0.05
E N-terminus
96
Mus NHE3
42
Rattus NHE3
99
Homo NHE3
62
Didelphis NHE3
Dasyatis NHE3
91
Triakis NHE3g
Triakis NHE3k/i
Danio NHE3a
Tribolodon NHE3
100
99
Danio NHE3b
0.05

Fig. 1. Isolation of NHE3k/i and NHE3g from banded houndshark *Triakis scyllium*. *A*: Schematic representation of NHE3k/i and NHE3g. Gray boxes indicate alternative amino termini of *Triakis* NHE3s and open boxes indicate the common region of *Triakis* NHE3s (749 amino-acid residues). Primers used for RT-PCR experiments are indicated by arrows. *B*: Expression of mRNAs encoding NHE3g, NHE3k/i, and β-actin in various tissues of houndshark. Semiquantitative RT-PCR was performed with primers in the common region (primers F1/R1) or isoform specific primers (F2/R2 and F3/R2). β-actin was used as an internal control for all cDNAs used in the analyses. *C*: Quantitative real-time RT-PCR analysis of NHE3g, NHE3k/i, and GAPDH in the gill, kidney, spiral intestine, and rectum. *D* and *E*: Phylogenetic analysis of NHE3s. Amino acid sequences of the common region of *Triakis* NHE3s (749 amino-acid residues) (*D*), and the alternative amino terminus (*E*) were compared with homologous regions of NHE3s of various species. Numbers indicate bootstrap values and scale bars represent a genetic distance of 0.05 amino-acid substitutions per site.

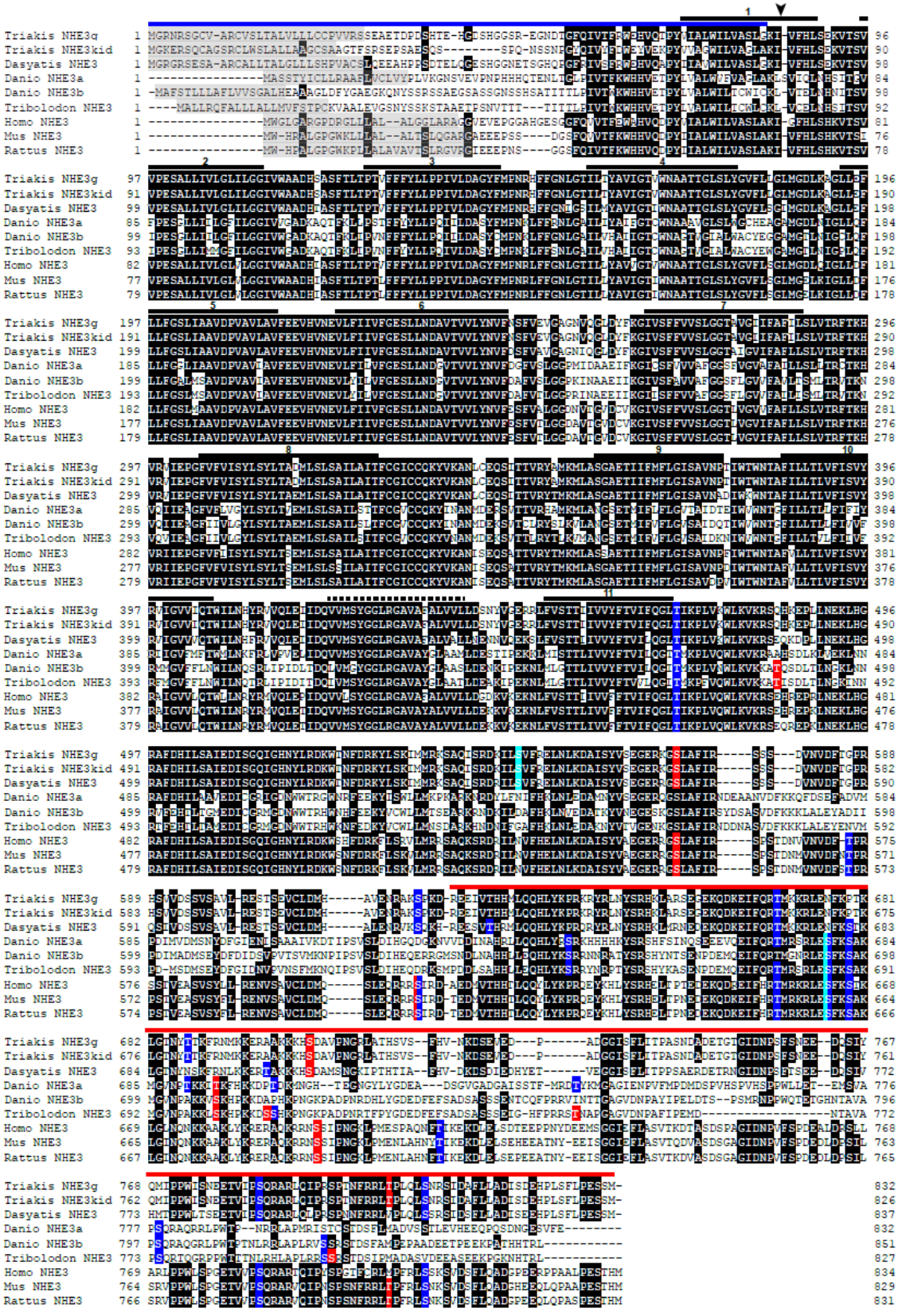
Triakis NHE3g
Triakis NHE3kid
Dasyatis NHE3
Danio NHE3a
Danio NHE3b
Tribolodon NHE3
Homo NHE3
Mus NHE3
Rattus NHE3

Fig. 2. Multiple alignment of NHE3. Blue line indicates the heterogeneous region between *Triakis* NHE3k/i and NHE3g. Red line indicates the fragment used for antibody preparation by Choe *et al.* (12). Conserved or semiconserved amino acid residues are shaded. Putative phosphorylation sites for PKA (-R/K-R/K-X-S/T-, where X is any amino acid (26, 48)), SGK (-R-x-R-x-x-S/T-Φ-, where X is any amino acid and Φ is hydrophobic (25, 40)), and PKC (-S/T-X-R/K-, where X is any amino acid (24)) are shown in red, cyan, and blue boxes, respectively. Presence of SGK in elasmobranch species was demonstrated in spiny dogfish (*Squalus acanthias*) by Waldegger et al. (52). Transmembrane domains are overlined and numbered, and an additional hydrophobic region is indicated by a dashed overline. Class I PDZ-binding motif at the carboxy termini (-S/T-X-Φ, where X is any amino acid and Φ is hydrophobic (17)) were conserved in *Triakis* NHE3k/i and NHE3g. Arrow head indicates the splice site of intron 1 in human, mouse, rat, and zebrafish NHE3 genes.

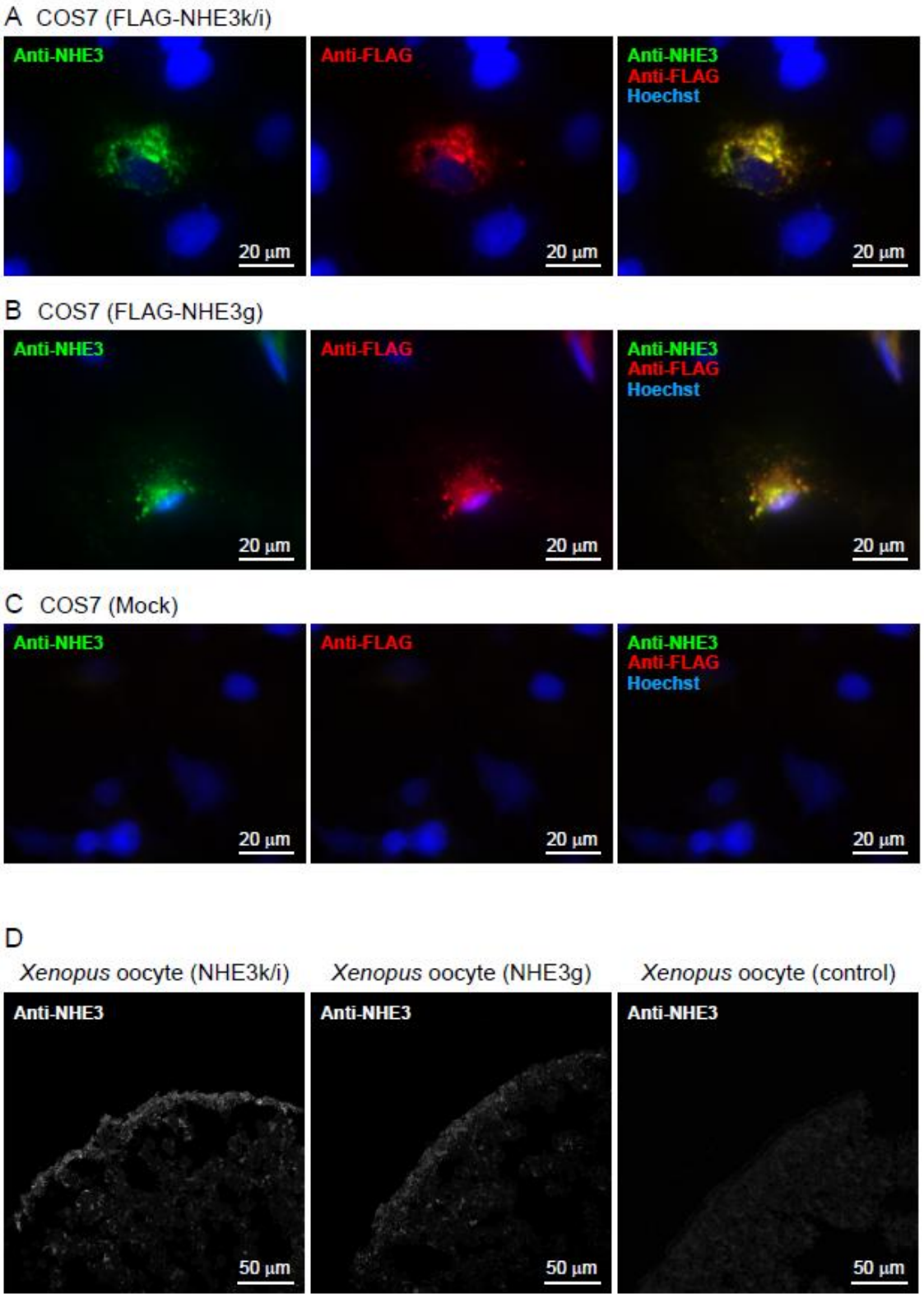
A COS7 (FLAG-NHE3k/i)
Anti-NHE3
Anti-FLAG
Anti-NHE3
Anti-FLAG
Hoechst
20 μm
B COS7 (FLAG-NHE3g)
C COS7 (Mock)
D
Xenopus oocyte (NHE3k/i)
Xenopus oocyte (NHE3g)
Xenopus oocyte (control)
50 μm

Fig. 3. Cross-reactivity of anti-NHE3 antibody. COS7 cells expressing 3×FLAG-NHE3k/i (A), 3×FLAG-NHE3g (B), or mock-transfected cells (C) were stained with anti-NHE3 (RIB2, green) and anti-FLAG (red) antibodies. Nuclei were stained with Hoechst 33342 (blue). *D*: Immunohistochemical analysis on *Xenopus* oocytes injected with cRNAs for NHE3k/i, NHE3g, or water.

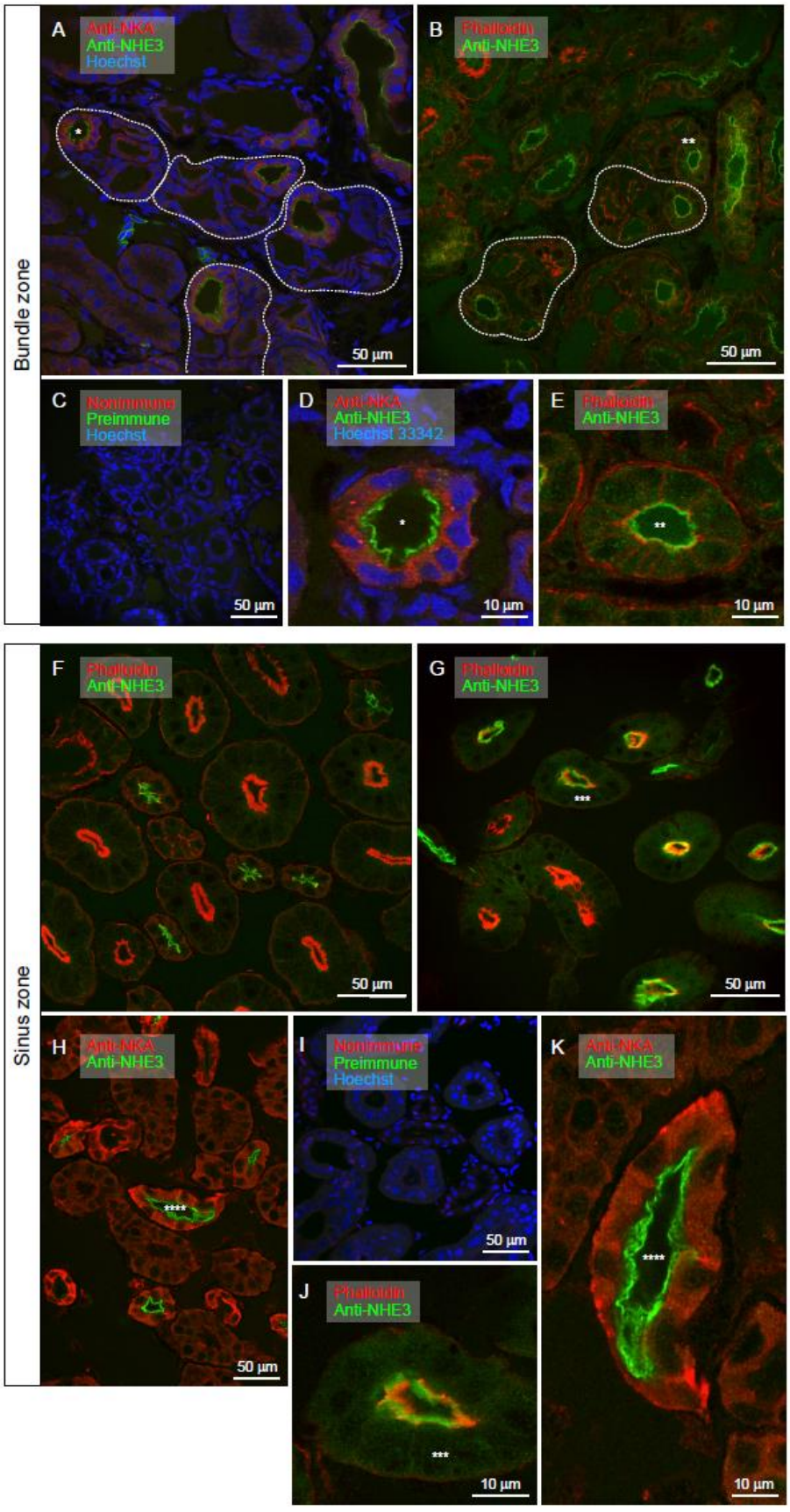
Bundle zone
A
Anti-NKA
Anti-NHE3
Hoechst
50 µm
B
Phalloidin
Anti-NHE3
50 µm
C
Nonimmune
Preimmune
Hoechst
50 µm
D
Anti-NKA
Anti-NHE3
Hoechst 33342
10 µm
E
Phalloidin
Anti-NHE3
10 µm
Sinus zone
F
Phalloidin
Anti-NHE3
50 µm
G
Phalloidin
Anti-NHE3
50 µm
H
Anti-NKA
Anti-NHE3
50 µm
I
Nonimmune
Preimmune
Hoechst
50 µm
J
Phalloidin
Anti-NHE3
10 µm
K
Anti-NKA
Anti-NHE3
10 µm

Fig. 4. Immunohistochemical analysis of NHE3k/i in the *Triakis* kidney. *A*–*E*: Expression of NHE3k/i in the bundle zone. *F*–*K*: Expression of NHE3k/i in the sinus zone. Confocal laser scanning micrographs of kidney slices stained with anti-NHE3 (green) and anti-Na^+/K^+-ATPase (red) are shown in *A*, *D*, *H*, and *K*. Images of the kidney sections stained with anti-NHE3 (green) and phalloidin (red) are shown in *B*, *E*, *F*, *G*, and *J*. No signals were observed in the preimmune serum (*C* and *I*). Asterisks indicate renal tubules, which are shown in high magnification views.

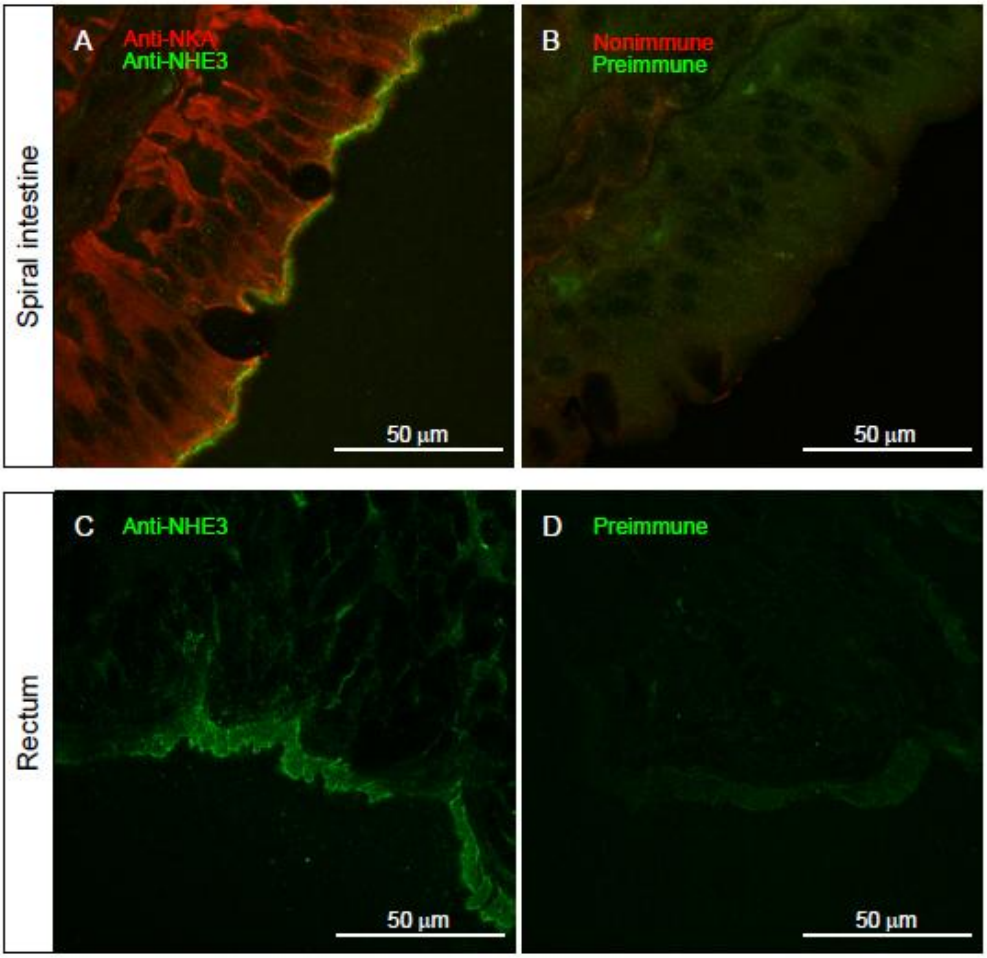

Fig. 5. Immunohistochemical analysis of NHE3k/i in the *Triakis* spiral intestine and rectum. *A* and *B*: Expression of NHE3k/i in the spiral intestine. *C* and *D*: Expression of NHE3k/i in the rectum. Confocal laser scanning micrographs of intestinal sections stained with anti-NHE3 (green) and anti-Na^+/K^+-ATPase (red) are shown in *A* and *C*. No signals were observed in the preimmune serum (*B* and *D*).

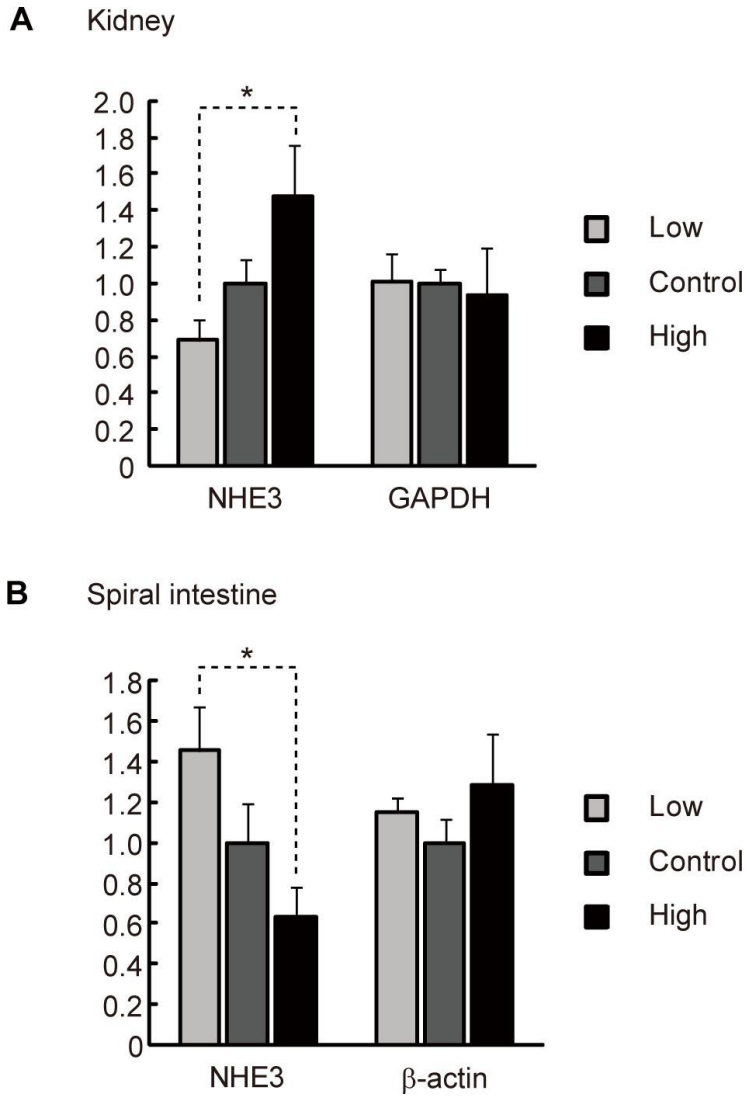

Fig. 6. Environmental salinity-dependent expression of NHE3 in the kidney and spiral intestine. Sharks were acclimated to 100% (Control), 60% (Low), or 130% seawater (High) for 2 days, and NHE3 mRNA expressions in the kidney (*A*) and spiral intestine (*B*) were determined by real-time PCR. Abundance of mRNA is shown as a ratio to those of the control animals. No significant differences were observed in GAPDH and β-actin expressions as positive controls for the renal and intestinal gene expressions, respectively. The asterisk indicates $p < 0.05$ by the Turkey-Kramer test. Values are expressed as means ± S.E. (n = 4–7).

Table 1. List of primers used for PCR amplification.

Gene	Sequence	Remark
NHE3	GCNGTKMTNGCNGTNTTYGARGA	Initial cloning (S)
	GCNCCNCKNARNCCNCCRTA	Initial cloning (AS)
	TGGAGCTGTAGCCTTTGCTT	RT-PCR (S), F1
	TATCGCACTGTGGATTCTGG	RT-PCR or qPCR (S), F2
	GAGAAGCCCTACGTTGTTGC	RT-PCR or qPCR (S), F3
	CTGCAGTGTTACGAGAGAGTACC	qPCR (S), F4
	TCTTGTTCTCGCCTTCACTG	RT-PCR (AS), R1
	CACATGCTTGGTGAATCTGG	RT-PCR (AS), R2
	TGGGTGGCAGGAGATAGAAG	qPCR (AS), R3
	GCTGTAATTAAGCCTGTACCGTTT	qPCR (AS), R4
	CCAGCATTTTCATGGCGTATCTG	5’ RACE (AS), R5 (outer)
	CTCACAGAGGTTGGCCTTTAC	5’ RACE (AS), R6
	ATGTCTGCTGTGAGGTAGGACA	5’ RACE (AS), R7
	CCTGCTCCTACTTCCACAAATG	5’ RACE (AS), R8 (inner)
	CCAGGAAACGGTACAGGCTTAATTACAG	3’ RACE (S), F5, (outer)
	TGGCGCGCAGTGAAGGCGAGAAACAA	3’ RACE (S), F6
	GGAACCAATTACACCACCAAATTTAGG	3’ RACE (S), F7 (inner)
	ATGGGCAAAGAGAGGAGCCAGTGTGCGGGC	ORF cloning (S), F8, NHE3k/i
	ATGGGGAGAAATAGGAGCGGCTGTGTGGCC	ORF cloning (S) , F9, NHE3g
	TTTACATTGATGATTCAGGTAGGAAAGACA	ORF cloning (AS) , R9, NHE3
β-actin	GCAAAACACCACACATTTCTCATAC	RT-PCR (S)
	ATGCCAATGAGTTGGTCGTCTA	RT-PCR (AS)
	CTCTTCTTCCCTTGAGAAGAGCTA	qPCR (S)
	CATGATTGAGTTGAAAGTGGTCTC	qPCR (AS)
GAPDH	CGCGTCCTGCACCACAA	qPCR (S)
	AATGCCAAAGTTATCCTCGATGA	qPCR (AS)

S, sense primer; AS, antisense primer. Degenerated primers were designed according to Choe et al. (12)

DISCUSSION

Molecular cloning and tissue distribution analyses of *Triakis* NHE3s clarified that two transcriptional isoforms, NHE3k/i and NHE3g, are generated from a single gene by alternative promoter usage (Fig. 1). The alternative amino termini may be have arisen by duplication of exon 1. Phylogenetic analyses (Fig. 1, *C* and *D*) and the low homology between the alternative amino termini suggest that the exon duplication was not a recent event but had occurred before separation of the shark and ray lineages. However, phylogenetic analysis provided no evidence when exon duplication had occurred before and after separation of the fish and tetrapod lineages. In zebrafish, two *nhe3* genes had been tandemly duplicated and generated *nhe3a* and *nhe3b* in chromosome 19 (57). *nhe3a* is highly expressed in the kidney with intermediate expression in the intestine, blood, and ovary, whereas *nhe3b* is expressed in several tissues including the gill (57). In the gill, elasmobranch NHE3g and zebrafish NHE3b are both localized in apical membrane of mitochondria-rich cells (12, 46, 57). Therefore, elasmobranch NHE3g and zebrafish NHE3b may have similar physiological functions, whereas elasmobranch NHE3k/i, zebrafish NHE3a, and mammalian NHE3 may be related to each other. In other words, both *Triakis* and zebrafish were found to have a pair of NHE3s in the gill and kidney/intestine that had arisen due to exon duplication (*Triakis*) or tandem gene duplication (zebrafish). When the two isoforms of NHE3 from *Triakis* were obtained, the question was whether the mechanism of their generation was division of gene expression resulting in subfunctionalization at the protein function level (6, 58).

Most of the *Triakis* NHE3s were localized intracellularly when expressed in *Xenopus* oocytes warranting further study to assess the activity of *Triakis* NHE3s in *Xenopus* oocytes and to elucidate any functional differences.

A previous study by Choe et al. noted that Atlantic stingray NHE3 is grouped closer to mammalian NHE3s than teleost NHE3s in a phylogenetic analysis, and suggested that NHE3 evolved rapidly in teleosts (12). Our present data also supported those results, i.e., *Triakis* NHE3s were more homologous to mammalian NHE3s than teleost NHE3s (Fig. 1*C*). Many phosphorylation sites are conserved in the carboxy-terminal cytoplasmic domain of NHE3s (Fig. 2), suggesting that NHE3s are regulated by phosphorylation in an identical manner.

Elasmobranch kidney is the site of urea retention, where 70–99% of filtered urea is reabsorbed (5, 9, 18). The renal tubules of elasmobranchs have a complex structure that consists of four loops. The mechanism of renal handling of urea, ions, and water is still largely unknown although urea transporter (20), ammonia transporter (37), Na^+-K^+-$2Cl^-$ cotransporter 2 (16), Na^+-glucose cotransporter 1 (3) and water channel aquaporins (14), have been identified and characterized in the elasmobranch kidney. The present immunohistochemical analysis of NHE3k/i in the kidney showed that NHE3k/i was expressed in the apical membrane of a part of the proximal tubules in the sinus zone (proximal III segment in the second loop as designated by Lacy and Reale), the early distal tubules in the bundle zone (intermediate IV segment of the third loop as designated by Lacy and Reale), and a part of the late distal tubules in the sinus zone (intermediate VI segment of the fourth loop as designated by Lacy and Reale) that expressed high levels of Na^+/K^+-ATPase in the basolateral

membrane(Fig. 4). Colocalization of NHE3k/i and Na^+/K^+-ATPase in renal segments indicates that NHE3k/i mediates Na^+ reabsorption and H^+ secretion using low intracellular Na^+ concentration as a driving force. In combination with vacuolar-type H^+-ATPase (V-ATPase) in the apical membrane of the proximal tubules (37), NHE3k/i may also contribute to urine acidification, which is advantageous for HCO_3^-/CO_2 reabsorption, NH_3/NH_4^+ reabsorption, Mg^{2+} excretion, and nutrient reabsorption. The level of NHE3k/i expression in the kidney of *Triakis* acclimated to 130% concentrated seawater was significantly higher than that in animals acclimated to 60% diluted seawater (Fig. 6*A*), suggesting that NHE3k/i is involved in renal Na^+ and H^+ regulation during hyperosmotic acclimation.

The role of intestine in osmoregulation and the mechanism of Na^+ and Cl^- absorption in elasmobranchs are not well understood. Moreover, the mechanism whereby luminal Na^+ and Cl^- are absorbed in the elasmobranch intestines is unknown. In mammals, luminal Na^+/H^+ exchangers (NHE3 and NHE2) and Cl^-/HCO_3^- exchangers (Slc26a6 and Slc26a3) mediate electroneutral NaCl absorption by the intestine. In seawater teleost, however, luminal Na^+-K^+-$2Cl^-$ cotransporter 2 (NKCC2) mediates salt absorption (13, 53), and the role of NHE3 in the intestine is not clear. Presence of NHE3k/i in the apical membrane of *Triakis* intestines (Fig. 1B and 5) suggests that the elasmobranch intestine has a Na^+ absorbing system similar to that of the mammalian intestine. Recently, drinking behavior and solutes in intestinal fluid have been studied in marine elasmobranchs (4-5). Elasmobranchs are able to gain water across the gill and therefore thought to have no need of drinking environmental water. However,

recent studies demonstrated that marine elasmobranchs drink environmental water when their blood volume is reduced after transferring to an environment of higher salinity (4-5). Interestingly, the level of NHE3k/i expression in the spiral intestine of *Triakis* acclimated to 130% seawater was significantly lower than that of animals acclimated to 60% seawater (Fig. 6*B*). In the intestine of bamboo shark (*Chiloscyllium plagiosum*), net influx rate of Na^+ was reduced significantly when the shark was acclimated to 140% seawater (5). These results suggest that NHE3k/i has less contribution on intestinal Na^+ absorption when drinking rate of seawater is increased. Salinity-dependent change in NHE3k/i expression was opposite between kidney and intestine, therefore, the kidney and intestine regulate NHE3 gene-expression differently.

REFERENCES

1. **American Physiological Society.** Guiding principles for research involving animals and human beings. *Am J Physiol Regul Integr Comp Physiol* 283:R281–R283, 2002.
2. **Aller SG, Lombardo ID, Bhanot S, and Forrest JN, Jr.** Cloning, characterization, and functional expression of a CNP receptor regulating CFTR in the shark rectal gland. *Am J Physiol* 276: C442-C449, 1999.
3. **Althoff T, Hentschel H, Luig J, Schutz H, Kasch M, and Kinne RK**. Na^+-D-glucose cotransporter in the kidney of *Squalus acanthias*: molecular identification and intrarenal distribution. *Am J Physiol Regul Integr Comp Physiol* 290: R1094-R1104, 2006.
4. **Anderson WG, Dasiewicz PJ, Liban S, Ryan C, Taylor JR, Grosell M, and Weihrauch D**. Gastro-intestinal handling of water and solutes in three species of elasmobranch fish, the white-spotted bamboo shark, *Chiloscyllium plagiosum*, little skate, *Leucoraja erinacea* and the clear nose skate *Raja eglanteria*. *Comp Biochem Physiol A Mol Integr Physiol* 155: 493-502, 2010.
5. **Anderson WG, Taylor JR, Good JP, Hazon N, and Grosell M**. Body fluid volume regulation in elasmobranch fish. *Comp Biochem Physiol A Mol Integr Physiol* 148: 3-13, 2007.
6. **Ayoubi TA, and Van De Ven WJ**. Regulation of gene expression by alternative promoters. *FASEB J* 10: 453-460, 1996.
7. **Brant SR, Yun CH, Donowitz M, and Tse CM**. Cloning, tissue distribution,

and functional analysis of the human Na^+/H^+ exchanger isoform, NHE3. *Am J Physiol* 269: C198-C206, 1995.

8. **Brett CL, Donowitz M, and Rao R**. Evolutionary origins of eukaryotic sodium/proton exchangers. *Am J Physiol Cell Physiol* 288: C223-C239, 2005.
9. **C. Bevan RKHK, R. E. Shetlar and E. Kinne-Saffran**. Presence of a Na^+/H^+ exchanger in brush border membranes isolated from the kidney of the spiny dogfish, *Squalus acanthias*. *J Comp Physiol B* 159: 339-347, 1989.
10. **Choe KP, Edwards SL, Claiborne JB, and Evans DH**. The putative mechanism of Na^+ absorption in euryhaline elasmobranchs exists in the gills of a stenohaline marine elasmobranch, *Squalus acanthias*. *Comp Biochem Physiol A Mol Integr Physiol* 146: 155-162, 2007.
11. **Choe KP, and Evans DH**. Compensation for hypercapnia by a euryhaline elasmobranch: effect of salinity and roles of gills and kidneys in fresh water. *J Exp Zool A Comp Exp Biol* 297: 52-63, 2003.
12. **Choe KP, Kato A, Hirose S, Plata C, Sindic A, Romero MF, Claiborne JB, and Evans DH**. NHE3 in an ancestral vertebrate: primary sequence, distribution, localization, and function in gills. *Am J Physiol Regul Integr Comp Physiol* 289: R1520-R1534, 2005.
13. **Cutler CP, and Cramb G**. Differential expression of absorptive cation-chloride-cotransporters in the intestinal and renal tissues of the European eel (*Anguilla anguilla*). *Comp Biochem Physiol B Biochem Mol Biol* 149: 63-73, 2008.

14. **Cutler CP, Maciver B, Cramb G, and Zeidel M**. Aquaporin 4 is a Ubiquitously Expressed Isoform in the Dogfish (*Squalus acanthias*) Shark. *Front Physiol* 2: 107, 2011.

15. **Esaki M, Hoshijima K, Kobayashi S, Fukuda H, Kawakami K, and Hirose S**. Visualization in zebrafish larvae of Na^+ uptake in mitochondria-rich cells whose differentiation is dependent on foxi3a. *Am J Physiol Regul Integr Comp Physiol* 292: R470-R480, 2007.

16. **Gagnon E, Forbush B, Flemmer AW, Gimenez I, Caron L, and Isenring P**. Functional and molecular characterization of the shark renal Na-K-Cl cotransporter: novel aspects. *Am J Physiol Renal Physiol* 283: F1046-F1055, 2002.

17. **Harris BZ, and Lim WA**. Mechanism and role of PDZ domains in signaling complex assembly. *J Cell Sci* 114: 3219-3231, 2001.

18. **Hazon N, Tierney, M. L., Anderson, G., Mackenzie, S., Cutler, C. and Cramb, G.** Ion and water balance in elasmobranch fish. In: *Ionic Regulation in Animals*, edited by Hazon N, Eddy FB, and Flik G. Berlin: Springer, 1997, p. 70-86.

19. **Hirata T, Kaneko T, Ono T, Nakazato T, Furukawa N, Hasegawa S, Wakabayashi S, Shigekawa M, Chang MH, Romero MF, and Hirose S**. Mechanism of acid adaptation of a fish living in a pH 3.5 lake. *Am J Physiol Regul Integr Comp Physiol* 284: R1199-R1212, 2003.

20. **Hyodo S, Katoh F, Kaneko T, and Takei Y**. A facilitative urea transporter is localized in the renal collecting tubule of the dogfish *Triakis scyllia*. *J Exp Biol* 207: 347-356, 2004.

21. **Hyodo S, Tsukada T, and Takei Y**. Neurohypophysial hormones of dogfish, *Triakis scyllium*: structures and salinity-dependent secretion. *Gen Comp Endocrinol* 138: 97-104, 2004.

22. **Kandasamy RA, and Orlowski J**. Genomic organization and glucocorticoid transcriptional activation of the rat Na^+/H^+ exchanger Nhe3 gene. *J Biol Chem* 271: 10551-10559, 1996.

23. **Kato A, Muro T, Kimura Y, Li S, Islam Z, Ogoshi M, Doi H, and Hirose S**. Differential expression of Na^+-Cl^- cotransporter and Na^+-K^+-Cl^- cotransporter 2 in the distal nephrons of euryhaline and seawater pufferfishes. *Am J Physiol Regul Integr Comp Physiol* 300: R284-R297, 2011.

24. **Kennelly PJ, and Krebs EG**. Consensus sequences as substrate specificity determinants for protein kinases and protein phosphatases. *J Biol Chem* 266: 15555-15558, 1991.

25. **Kobayashi T, and Cohen P**. Activation of serum- and glucocorticoid-regulated protein kinase by agonists that activate phosphatidylinositide 3-kinase is mediated by 3-phosphoinositide-dependent protein kinase-1 (PDK1) and PDK2. *Biochem J* 339 (Pt 2): 319-328, 1999.

26. **Kocinsky HS, Girardi AC, Biemesderfer D, Nguyen T, Mentone S, Orlowski J, and Aronson PS**. Use of phospho-specific antibodies to determine the phosphorylation of endogenous Na^+/H^+ exchanger NHE3 at PKA consensus sites. *Am J Physiol Renal Physiol* 289: F249-258, 2005.

27. **Kumai Y, and Perry SF**. Ammonia excretion via Rhcg1 facilitates Na^+

uptake in larval zebrafish, *Danio rerio*, in acidic water. *Am J Physiol Regul Integr Comp Physiol* 301: R1517-R1528, 2011.

28. **Kurita Y, Nakada T, Kato A, Doi H, Mistry AC, Chang MH, Romero MF, and Hirose S**. Identification of intestinal bicarbonate transporters involved in formation of carbonate precipitates to stimulate water absorption in marine teleost fish. *Am J Physiol Regul Integr Comp Physiol* 294: R1402-R1412, 2008.
29. **Lacy ER, and Reale E**. The elasmobranch kidney. II. Sequence and structure of the nephrons. *Anat Embryol (Berl)* 173: 163-186, 1985.
30. **Lehrich RW, Aller SG, Webster P, Marino CR, and Forrest JN, Jr.** Vasoactive intestinal peptide, forskolin, and genistein increase apical CFTR trafficking in the rectal gland of the spiny dogfish, *Squalus acanthias*. Acute regulation of CFTR trafficking in an intact epithelium. *J Clin Invest* 101: 737-745, 1998.
31. **Lin CC, Lin LY, Hsu HH, Thermes V, Prunet P, Horng JL, and Hwang PP**. Acid secretion by mitochondrion-rich cells of medaka (*Oryzias latipes*) acclimated to acidic freshwater. *Am J Physiol Regul Integr Comp Physiol* 302: R283-291, 2012.
32. **Lin TY, Liao BK, Horng JL, Yan JJ, Hsiao CD, and Hwang PP**. Carbonic anhydrase 2-like a and 15a are involved in acid-base regulation and Na^+ uptake in zebrafish H^+-ATPase-rich cells. *Am J Physiol Cell Physiol* 294: C1250-C1260, 2008.
33. **Mahnensmith RL, and Aronson PS**. The plasma membrane sodium-hydrogen exchanger and its role in physiological and

pathophysiological processes. *Circ Res* 56: 773-788, 1985.

34. **Marshall WS, and Grosell M**. Ion transport, osmoregulation, and acid-base balance. In: *The Physiology of Fishes*, edited by Evans DH, and Claiborne JB. New York: CRC, 2005, p. 177-224.

35. **Mistry AC, Honda S, Hirata T, Kato A, and Hirose S**. Eel urea transporter is localized to chloride cells and is salinity dependent. *Am J Physiol Regul Integr Comp Physiol* 281: R1594-R1604, 2001.

36. **Nakada T, Hoshijima K, Esaki M, Nagayoshi S, Kawakami K, and Hirose S**. Localization of ammonia transporter Rhcg1 in mitochondrion-rich cells of yolk sac, gill, and kidney of zebrafish and its ionic strength-dependent expression. *Am J Physiol Regul Integr Comp Physiol* 293: R1743-R1753, 2007.

37. **Nakada T, Westhoff CM, Yamaguchi Y, Hyodo S, Li X, Muro T, Kato A, Nakamura N, and Hirose S**. Rhesus glycoprotein p2 (Rhp2) is a novel member of the Rh family of ammonia transporters highly expressed in shark kidney. *J Biol Chem* 285: 2653-2664, 2010.

38. **Orlowski J, and Grinstein S**. Diversity of the mammalian sodium/proton exchanger SLC9 gene family. *Pflugers Arch* 447: 549-565, 2004.

39. **Orlowski J, Kandasamy RA, and Shull GE**. Molecular cloning of putative members of the Na/H exchanger gene family. cDNA cloning, deduced amino acid sequence, and mRNA tissue expression of the rat Na/H exchanger NHE-1 and two structurally related proteins. *J Biol Chem* 267: 9331-9339, 1992.

40. **Park J, Leong ML, Buse P, Maiyar AC, Firestone GL, and Hemmings**

BA. Serum and glucocorticoid-inducible kinase (SGK) is a target of the PI 3-kinase-stimulated signaling pathway. *EMBO J* 18: 3024-3033, 1999.

41. **Pathak BG, Shull GE, Jenkins NA, and Copeland NG**. Mouse chromosomal location of four Na/H exchanger isoform genes. *Genomics* 31: 261-263, 1996.
42. **Romero MF, Fong P, Berger UV, Hediger MA, and Boron WF**. Cloning and functional expression of rNBC, an electrogenic Na^+-HCO_3^- cotransporter from rat kidney. *Am J Physiol* 274: F425-F432, 1998.
43. **Saitou N, and Nei M**. The neighbor-joining method: a new method for reconstructing phylogenetic trees. *Mol Biol Evol* 4: 406-425, 1987.
44. **Schultheis PJ, Clarke LL, Meneton P, Harline M, Boivin GP, Stemmermann G, Duffy JJ, Doetschman T, Miller ML, and Shull GE**. Targeted disruption of the murine Na^+/H^+ exchanger isoform 2 gene causes reduced viability of gastric parietal cells and loss of net acid secretion. *J Clin Invest* 101: 1243-1253, 1998.
45. **Shih TH, Horng JL, Liu ST, Hwang PP, and Lin LY**. Rhcg1 and NHE3b are involved in ammonium-dependent sodium uptake by zebrafish larvae acclimated to low-sodium water. *Am J Physiol Regul Integr Comp Physiol* 302: R84-R93, 2012.
46. **Takabe S, Teranishi K, Takaki S, Kusakabe M, Hirose S, Kaneko T, and Hyodo S**. Morphological and functional characterization of a novel Na^+/K^+-ATPase-immunoreactive, follicle-like structure on the gill septum of Japanese banded houndshark, Triakis scyllium. *Cell Tissue Res* 348: 141-153, 2012.

47. **Tamura K, Peterson D, Peterson N, Stecher G, Nei M, and Kumar S**. MEGA5: molecular evolutionary genetics analysis using maximum likelihood, evolutionary distance, and maximum parsimony methods. *Mol Biol Evol* 28: 2731-2739, 2011.

48. **Taylor SS, Buechler JA, and Yonemoto W**. cAMP-dependent protein kinase: framework for a diverse family of regulatory enzymes. *Annu Rev Biochem* 59: 971-1005, 1990.

49. **Tran YH, Xu Z, Kato A, Mistry AC, Goya Y, Taira M, Brandt SJ, and Hirose S**. Spliced isoforms of LIM-domain-binding protein (CLIM/NLI/Ldb) lacking the LIM-interaction domain. *J Biochem* 140: 105-119, 2006.

50. **Tse CM, Brant SR, Walker MS, Pouyssegur J, and Donowitz M**. Cloning and sequencing of a rabbit cDNA encoding an intestinal and kidney-specific Na^+/H^+ exchanger isoform (NHE-3). *J Biol Chem* 267: 9340-9346, 1992.

51. **Tsui TK, Hung CY, Nawata CM, Wilson JM, Wright PA, and Wood CM**. Ammonia transport in cultured gill epithelium of freshwater rainbow trout: the importance of Rhesus glycoproteins and the presence of an apical $Na^+/NH4^+$ exchange complex. *J Exp Biol* 212: 878-892, 2009.

52. **Waldegger S, Barth P, Forrest JN, Jr., Greger R, and Lang F**. Cloning of sgk serine-threonine protein kinase from shark rectal gland - a gene induced by hypertonicity and secretagogues. *Pflugers Arch* 436: 575-580, 1998.

53. **Watanabe S, Mekuchi M, Ideuchi H, Kim YK, and Kaneko T**. Electroneutral cation-Cl^- cotransporters NKCC2β and NCCβ expressed in the intestinal tract of Japanese eel *Anguilla japonica*. *Comp Biochem*

Physiol A Mol Integr Physiol 159: 427-435, 2011.

54. **Wingert RA, Selleck R, Yu J, Song HD, Chen Z, Song A, Zhou Y, Thisse B, Thisse C, McMahon AP, and Davidson AJ**. The cdx genes and retinoic acid control the positioning and segmentation of the zebrafish pronephros. *PLoS Genet* 3: 1922-1938, 2007.

55. **Xie Q, Welch R, Mercado A, Romero MF, and Mount DB**. Molecular characterization of the murine Slc26a6 anion exchanger: functional comparison with Slc26a1. *Am J Physiol Renal Physiol* 283: F826-F838, 2002.

56. **Yamaguchi Y, Takaki S, and Hyodo S**. Subcellular distribution of urea transporter in the collecting tubule of shark kidney is dependent on environmental salinity. *J Exp Zool A Ecol Genet Physiol* 311: 705-718, 2009.

57. **Yan JJ, Chou MY, Kaneko T, and Hwang PP**. Gene expression of Na^+/H^+ exchanger in zebrafish H^+ -ATPase-rich cells during acclimation to low-Na^+ and acidic environments. *Am J Physiol Cell Physiol* 293: C1814-C1823, 2007.

58. **Zhang J**. Evolution by gene duplication: an update. *Trends Ecol Evol* 18: 7, 2003.

ACKNOWLEDGMENTS

First of all, I would like to express my grateful to Professor Shigehisa Hirose for his supervision and encouragement. I am very grateful to Assistant Professor Akira Kato for his technical support, instruction, and suggestion; and Associate Professor Susumu Hyodo, Dr. Souichirou Takabe, Professor Michael F. Romero, Dr. An-Ping Chen, Takahiro Umezawa, and Dr. Tsutomu Nakada for collaboration. I thank Associate Professor Nobuhiro Nakamura and colleagues in Professor Hirose's laboratory for their help and cooperation. I also would like to thank Dr. Keith P. Choe for providing the anti-NHE3 antibody; Dr. Min-Hwang Chang and Dr. Taku Hirata for helpful suggestions; Yayoi Ueno and Heather L. Holmes for their technical assistance; Yoko Yamamoto, Ayako Takada, and Nana Shinohara for performing the DNA sequence analysis; and Yuriko Ishii for her secretarial assistance. Finally, I would like to express my gratefulness to my family and all my friends for their encouragement.

The main part of this thesis has been published in the *American Journal of Physiology - Regulatory, Integrative and Comparative Physiology* (vol. 304, no. 10, pp. R865- R876, 2013). Use of the article in the present thesis is permitted by the American Physiological Society.

This work was supported by the Ministry of Education, Culture, Sports, Science and Technology of Japan (MEXT) Grants-in-Aid for Scientific Research 21770077, 22370029, 21570061, Global Center of Excellence Program of MEXT, and the Sumitomo Foundation (100535). Work in the Romero lab was supported

by the NIH (EY017732, DK083007, and DK090728). I was supported by Monbukagakusho（MEXT) scholarship from Japan Government.